Impact of Process Parameters on Critical Performance Attributes of a Continuous Blender—A DEM-Based Study

Atul Dubey, Aditya U. Vanarase, and Fernando J. Muzzio
Dept. of Chemical and Biochemical Engineering, Rutgers University, Piscataway, NJ 08854

DOI 10.1002/aic.13770
Published online March 12, 2012 in Wiley Online Library (wileyonlinelibrary.com).

A discrete element method-based computational study carried out to study the effect of impeller design, speed, and input feed rate on the performance of a continuous powder blender is presented. The blender performance was characterized using the mean particle residence time, the residence time distribution, the number of blade passes experienced by the powder, and the mean centered variance. The powder residence time decreased with increasing impeller speed; however, the number of blade passes experienced a maximum at an intermediate speed. The effects of feed rate and impeller design were more prominent at lower speeds. Lower feed rate resulted in the powder experiencing higher number of blade passes. The number of blade passes was also higher for the alternate blade pattern when compared to the forward pattern. The computational findings were compared with an experimental study which showed that the model captured the essential flow dynamics well. © 2012 American Institute of Chemical Engineers *AIChE J,* 58: 3676–3684, 2012
Keywords: continuous blender, discrete element method, residence time distribution

Introduction

Granular mixing has been a subject of keen interest in the past decades. Even though there is a need for homogeneous mixtures in a vast number of industrial processes, the current understanding of the underlying phenomena leaves much to be desired. Time and cost efficient production of powder mixtures is a critical step in many industries such as pharmaceuticals, cosmetics, food, and so forth. Different application areas allow different degrees of allowance in terms of blend homogeneity and relevant sample size. Quality control requirements are especially stringent in areas such as pharmaceutical manufacturing. In this case, the mixing problem is compounded, as many of the ingredients have poor flow properties and exhibit segregation and/or agglomeration at the finished product scale (typically one tablet or one capsule). Furthermore, the formulations require low concentrations of active pharmaceutical ingredients in many dosage forms.[1] It is, therefore, extremely important to have a good understanding of the mixing mechanisms and the effect of various material- and process variables. With continuous processes gaining popularity in recent years, it is imperative to apply experiment and model-based approaches to identify optimal operating conditions for their effective design and operation.

Numerical modeling and simulation techniques have been applied to study mixing mechanisms in many types of blenders such as the V-Blender[2–4] the Tote blender,[5,6] the Double Cone blender,[2,7] continuous blender,[8] and a simple rotating drum.[9] Several other types of mixing processes have been studied using computational techniques.[3,9–15] These methods predominantly use discrete element modeling (DEM) to simulate flow and mixing, although other methods such as continuum modeling,[16–18] and Markov chain modeling,[19–21] data based methods,[22] and compartment modeling[23] have also been used in certain cases. DEM simulations have been shown to have good agreement with experimental studies of mixing using techniques such as Positron emission particle tracking[24,25] in batch mixers such as the V-blender[26] and simple rotating cylinder.[27,28] A relatively recent body of work is available in the area of continuous mixing.[8,22,29–32]

This article presents a study of a continuous blender aimed at its performance characterization under varying operating conditions. The aim is to establish and use a predictive model with the use of DEM techniques validated by experimental analysis. This particular study focuses on the effect of impeller speed, input feed rate (process parameters), and impeller blade type (a design parameter) on the performance of a commercial mixer. Experimental data from the same blender is used to validate the results.

The remainder of this article is organized in the following way. Computational Study section describes the computer simulation methodology; Results section presents the simulation results and the method validation. The Conclusions and Discussion section contains a summary of key conclusions and discussion. In summary, the simulations showed that for this blender, an increase in impeller speed leads to a reduction in the mean residence time and the narrowing of residence time distribution (RTD) curves. The number of blade passes and mean centered variance go through a peak with increasing impeller speed. An increase in feed rate leads to a decrease in mean residence time, narrowing of RTD, and a decrease in the number of blade passes. Using the alternating

Correspondence concerning this article should be addressed to F. J. Muzzio at fjmuzzio@yahoo.com.

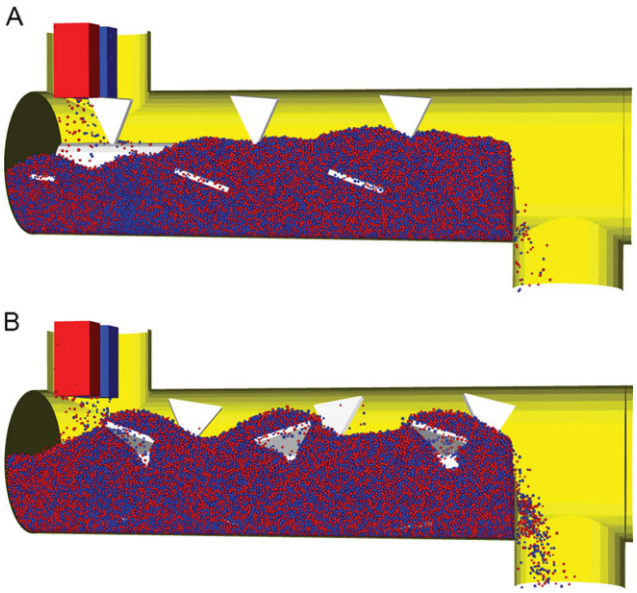

Figure 1. Simulation of a Gericke™ continuous blender.

Two feeders continuously provide particles in two streams on either side of the impeller which rotates counter clockwise when seen from the inlet side. (A) Forward impeller blade pattern and (B) alternating forward–backward pattern. [Color figure can be viewed in the online issue, which is available at wileyonlinelibrary.com.]

impeller blade pattern results in higher mean residence times, wider RTDs, and a higher number of blade passes.

Computational Study

Simulation method

Computer simulations of the solids mixing process were performed using DEM, a method developed originally by Cundall and Strack.[33] For maximum accuracy, computer aided drawings of the blender with 1:1 size ratio were created using Pro/Engineer software. The drawings were imported into a commercial DEM-based simulation program called EDEM™ (DEM Solutions Ltd.). At the inlet of the blender were two feeders providing a continuous supply of particles on either side of the impeller at a uniform feed rate (Figure 1). The two free flowing particle streams were introduced completely segregated from each other. The outlet of the blender features a semicircular weir that is used to increase the holdup and facilitate back mixing. The weir was placed such that its straight edge made a 45° angle with the horizontal. The impeller rotation was counterclockwise when viewed along the axis of rotation from the inlet end. Based on previous work[23,30,34,35] two impeller blade patterns were designed using the blade angles shown in Table 1. The first pattern had 12 blades with all forward facing (in the direction of flow) angles except for the last blade (Figure 1A) and the second pattern had 12 blades with alternating forward–reverse angles (Figure 1B). The angles were measured relative to the axis of rotation of the impeller. The simulation parameters are detailed in Table 2. An integration time step of 2.17e–05 s. was used. The input feed rate was varied between 15, 30, and 45 kg/h and six impeller speeds (40, 100, 130, 160, 205, and 250 rpm) were used in this study.

Table 1. Impeller Blade Patterns

Impeller Blade Pattern Name	Blade Angles (deg.)
Forward-blades pattern	5, 20, 20
	20, 20, 20
	20, 20, 20
	20, 20, -30
Alternating-blades pattern	5, 20, 20
	−20, 20, 20
	20, -20, 20
	−20, 20, -30

Typical particle numbers at steady state in the blender ranged from 20,000 to 350,000 going down in speed from 250 to 40 rpm.

Computational model

DEM is widely used for the simulation of granular phenomena. This study uses a damped contact model introduced by Tsuji et al.,[36] which is based on Hertzian contact theory[37] along with a Mindlin-Deresiewicz[38] tangential force model. The distance between the centers of each pair of particles or between particles and boundaries is computed at every time step. A contact is detected if the distance between the centers of particles (in case of a particle–particle contact) is less than sum of the particle radii or the distance between a boundary and the center of a particle (in case of a particle–boundary contact) is less than the particle radius.

Complete details of the force model are not reproduced here but are available in Dubey et al.[8] This contact model is incorporated in a commercial DEM modeling software package, EDEM™ (DEM Solutions Ltd.) and has been shown to provide good agreement with experimental studies involving bladed mixers,[8,39] size-segregation studies,[40] bulk solids mixing and conveying,[41] and fluidized bed reactors.[42,43] It has been shown to be comparable to other popular models.[44,45]

Results

Data acquisition and processing

The blender run was simulated until the mass holdup in the blender reached a near-constant value, indicating that a steady state has been achieved. The RTD was measured in

Table 2. DEM Simulation Parameters

Particle properties	Shear modulus: 2e+06 N/m^2
	Poisson's Ratio: 0.25
	Density: 1500 kg/m^3
	Average diameter: 2 mm
	Normal size distribution with SD = 0.2
Particle–particle interactions	Coefficient of static Friction : 0.5
	Coefficient of rolling friction : 0.01
	Coefficient of restitution: 0.4
Blender walls	Material: glass
	Shear modulus: 26 GPa
	Density: 2200 kg/m^3
	Poisson's ratio: 0.25
Blades	Material: steel
	Shear modulus: 80 GPa
	Density: 7800 kg/m^3
	Poisson's ratio: 0.29
Particle–blade interactions	Coefficient of static friction: 0.5
	Coefficient of rolling friction: 0.01
	Coefficient of restitution: 0.5
Particle–wall interactions	Coefficient of static friction: 0.5
	Coefficient of rolling friction: 0.01
	Coefficient of restitution: 0.5

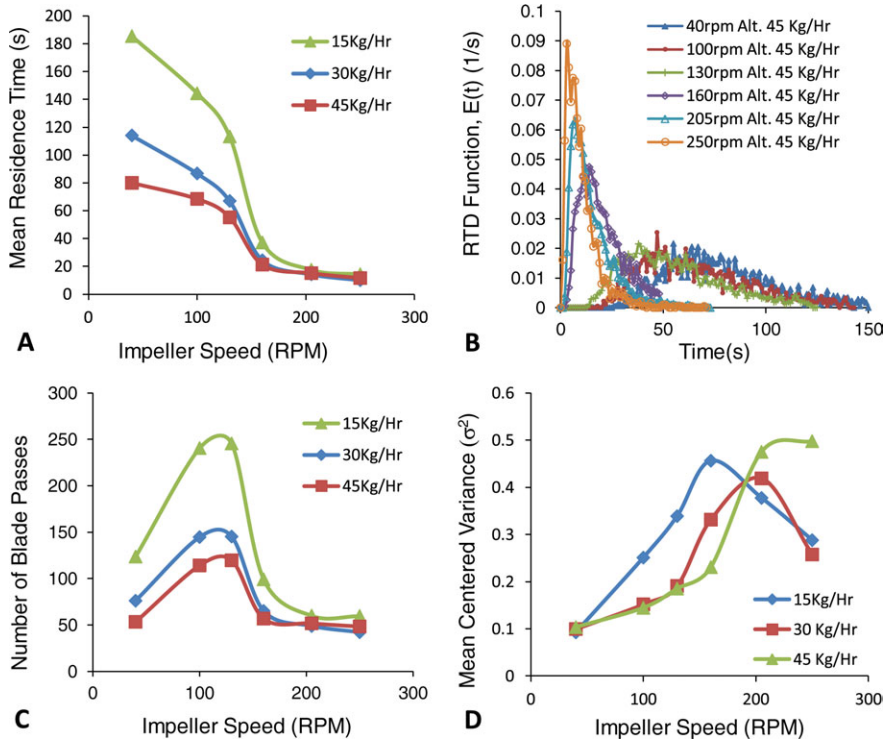

Figure 2. Effect of impeller speed on (A) mean residence time; (B) RTD; (C) number of blade passes; and (D) mean centered variance.

[Color figure can be viewed in the online issue, which is available at wileyonlinelibrary.com.]

the following way. After the steady state was achieved, the particles that were fed to the blender within a 1-s window were tagged. These particles were tracked until they crossed the weir at the outlet of the mixer. The time taken by each tagged particle to cross the weir was recorded as the residence time of the particle. The simulations were run at steady state for time intervals long enough so that at least 95% of the tagged particles were retrieved at the outlet. A histogram was created using 1-s time bins and the number of particles in each time bin [$c(t)$] was plotted against time. The RTD function, $E(t)$, was calculated by normalizing the area under the t–$c(t)$ curve.

It can be mathematically expressed as

$$E(t) = \frac{c(t)}{\int_0^\infty c(t).dt} \tag{1}$$

Taking an integral of the first moment of the RTD function yields the mean residence time, τ.

$$\tau = \int_0^\infty t.E(t).dt \tag{2}$$

Knowledge of the residence time leads to the amount of shear the material experiences in the blender, given by the number of blade passes (N_p). It is a function of the impeller rotation rate ω and the residence time τ

$$N_p = \omega * \tau \tag{3}$$

Finally, the mean centered variance is given by

$$\sigma_\tau^2 = \frac{\int_0^\infty (t-\tau)^2.E(t).dt}{\tau^2} \tag{4}$$

Experimental method. Experiments were performed using a Gericke™ GCM250 blender with similar geometry to the one used in the simulations. The impeller speeds, feed rates, and blade designs were also kept the same. Fast Flo™ lactose was used as the feed material. RTDs were measured by giving an impulse of a tracer (Acetaminophen) and measuring the tracer concentration at the blender discharge as a function of time. The tracer concentration [$c(t)$] was used in a similar way as described for the computational method to derive τ, $E(t)$, N_p, and σ^2. Complete details of the experimental procedure can be found in Vanarase and Muzzio.[46]

The following results in this section are organized with respect to the observed effects in relation to changes in parameters. First, the effect of variation in impeller speed on mean residence time, number of blade passes, and the RTD will be presented followed by the effects of change in feed rate and impeller design on the same. The effects of speed and feed rate were not independent of each other and hence will be discussed in parallel whenever necessary.

Effect of impeller speed. The powder dynamics inside the blender and the output blend quality are affected by the impeller rotation speed. Higher speeds can create fluidization, whereas lower speeds may not. Speed affects the time spent by the powder inside the blender; and consequently, the rate and amount of shear that it experiences through the impeller blades. The effect of impeller speed on mean residence time (τ), which is calculated using Eq. 2, is shown in Figure 2A. The material hold up (and consequently the

residence time) decreases nonlinearly with increasing impeller speed. It is evident that two different regimes exist in the system. The first three points (40, 100, and 130 rpm—before fluidization) are grouped together and are separated from the last three points (postfluidization), which display an abrupt and substantial decrease in the residence time, due to a corresponding abrupt decrease in the amount of powder present in the blender (holdup) that has also been observed experimentally. This difference is evidently more pronounced at the lowest feed rate where the rate of change of τ at prefluidization speeds was the sharpest. The mean residence time values for all feed rates are comparable at speeds of more than 160 rpm. Higher speed diminishes the effect of change in feed rate showing that the feed rate (within the given range) ceases to be important (in terms of affecting the bulk movement) at high speeds. The take home message is that if the mixer is to be operated at nonfluidized state and a scale up/down is desired, the change in feed rate must be accompanied by a corresponding change in impeller rotation speed to achieve comparable τ.

The effect of impeller speed on the RTD at a feed rate of 45 kg/h is shown in Figure 2B. The RTD function $E(t)$ provides a quantitative measurement of the behavior of a tracer which is modeled as a set of particles introduced into the blender in a 1-s time window. The RTD is also the fundamental characteristic controlling macromixing performance in a continuous mixer.[34,47,48] The plots show that a large fraction of the tracer particles spent a small amount of time in the blender at high impeller speeds. The distributions at speeds less than 130 rpm show that some particles spend a long time (>100 s) in the blender, whereas some spend relatively less time (<50 s). Importantly, Figure 2B shows once again two distinct groups of RTDs, at low speeds and at high speeds, once again reflecting the fluidization transition that occurs in this system around 160 rpm.

The amount of shear experienced by the powder as it travels through the blender can have a marked effect on the process design especially when a lubricant such as magnesium stearate is present in the blend which is known to make the blend more hydrophobic when high amount of shear is applied to it. Hydrophobicity affects the dissolution properties of the tablets thus produced.[49,50] Figure 2C shows the number of blade passes experienced by the powder when passing through the blender which is a combined effect of the impeller speed and the residence time (Eq. 3). The number of blade passes increases from 40 to 130 rpm but decrease thereafter. This shows that the maximum amount of shear on the powder will be imparted in the intermediate speeds near 130 rpm. The number of blade passes at speeds of 160 rpm and higher were comparable to that at 40 rpm.

The mean centered variance (σ^2), which provides a quantitative measure of the amount of dispersion (backmixing) produced by the mixer (Eq. 4), shows slightly different behavior with increasing impeller speed at the three feed rates (Figure 2D). The dispersion produced at the lowest speed was comparable at all feed rates. At the lowest feed rate, the mean centered variance then increased with speed up to 160 rpm; beyond which it decreased, indicating that the blender causes more dispersion at 160 rpm than at 205 rpm or 250 rpm. At the intermediate feed rate, however, the variance increased up to 205 rpm and the decrease came only after that. At the highest feed rate, it does not decrease at all but plateaus out at 205 rpm. As the mean centered variance is directly proportional to the dispersion coefficient, and thus, it indicates the amount of backmixing present in the system, these results indicate the presence of a strong interaction between impeller speed and flow rate in the mixer. Selection of optimum process parameters, and the development of dynamic models to be used for control purposes must be approached with care.

Effect of feed rate. The powder feeding rate into the blender (typically from loss-in-weight feeders) is also an important process parameter. Pharmaceutical blends may require multiple ingredients fed by different feeders. If a change in formulation or scale up/down is desired, the feed rate(s) have to be altered. Understanding the effect this might have is critical for quality control. Figure 3 shows the effect of feed rate on the mean residence time and the RTD. When the blender is operating in a nonfluidized regime, increasing feed rate leads to a reduction in the mean residence time. However, as seen in Figure 3A, the effect is less (or nonexistent) at higher speeds. The RTD function $E(t)$ (Figure 3B) shows a leftward drift with increasing feed rate. At 40 and 160 rpm, the distributions also become narrower with increasing feed rate. This shows that while the average time spent by the powder is higher at lower feed rates, the variability in the amount of shear will also be higher. This effect is diminished at higher speeds. As shown in Figure 3C, at 160 rpm when fluidization has just begun, the profiles at 30 and 45 kg/h are similar to each other but the lowest feed rate is still different. There is a significant portion of material that is spending a longer amount of time in the blender. At speeds postfluidization, the profiles tend to be more similar at different feed rates (Figure 3D). This shows that at high speeds, not only are the mean residence times comparable for all feed rates but also their distributions as similar as well. In other words, at high impeller speeds, powder holdup increases roughly proportionally to feed rate, giving mixing performance that is nearly independent of feed rate. This is an important observation that indicates that at such higher speeds, mixing performance is robust with respect to changes in feed rate, which is very useful for control purposes. This observation confirms similar findings by Portillo for a different continuous mixer,[30] and before that by Sudah et al.[48] for a rotary calciner.

The number of blade passes (N_p) exhibit a decreasing trend with increasing feed rate in general (Figure 4A). Interestingly, the numbers at 100 and 130 rpm are similar at all feed rates and the curves sit distinctly higher than the rest. Feed rate had little or no effect at 205 and 250 rpm. It must be noted that as shown in Figure 2C, the N_p peaks are in the 100–130 rpm range, and where, presumably, homogenization must be maximized. At 40, 160, 205, and 250 rpm, the highest feed rate produced similar number of blade passes, that is, under these conditions, the higher feed rate compensated for the effect of speed. However, the similar number of blade passes is applied at widely different shear rates and under very different powder flow regimes, with a very likely impact on micromixing behavior.

The mean centered variance (Figure 4B) increases with feed rate at high speeds (>200 rpm) and decreases for all other speeds except for the lowest one. Hence, it can be inferred that the powder is likely to receive more shear at the speeds of 40, 100, 130, and 160 rpm when fed at a lower feed rate.

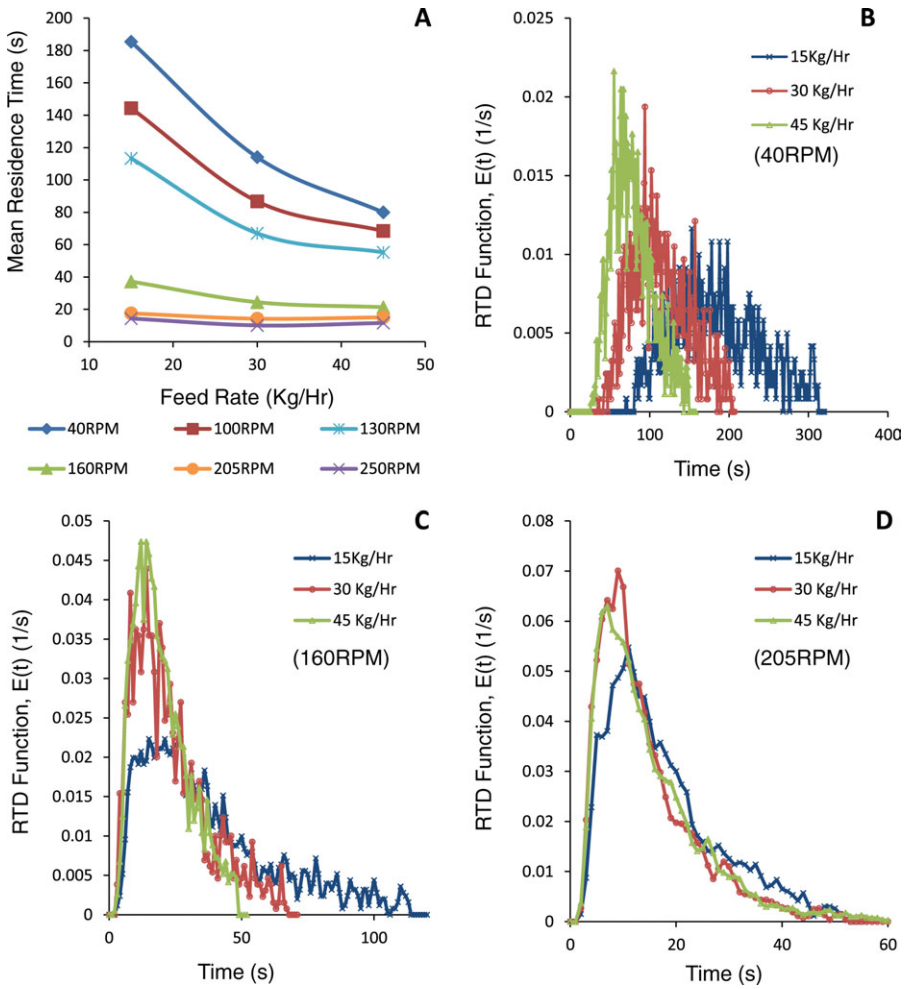

Figure 3. Effect of feed rate on (A) mean residence time; (B) RTD at low speed (40 rpm); (C) RTD when fluidization starts (160 rpm); and (D) RTD postfluidization.

[Color figure can be viewed in the online issue, which is available at wileyonlinelibrary.com.]

Effect of impeller blade pattern. The effect of change in impeller design on the mean residence time is shown in Figure 5A. The alternating-blade pattern resulted in higher holdup and mean residence time values compared to the forward-blade design. The plot shows that the back mixing due to backward facing blades continues to have an effect at all speeds. However, the effect is diminished at 250 rpm as the two curves tend to converge.

Even though the mean residence times get closer with increasing speed, the RTDs are different. Figures 5B,C show

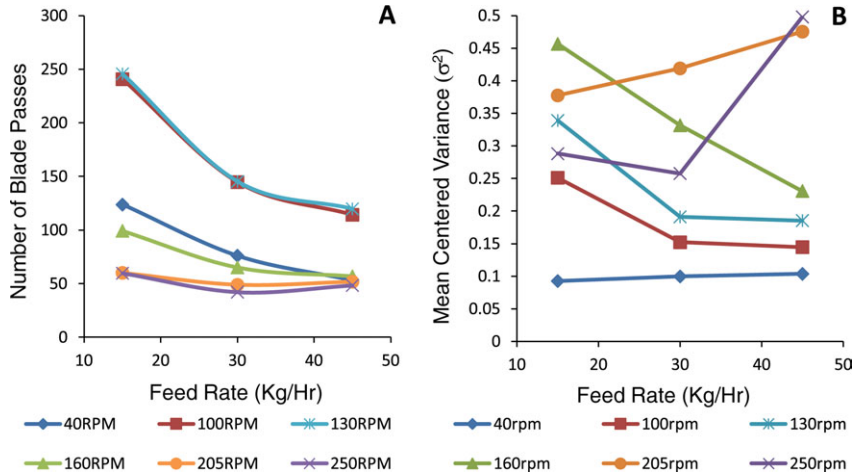

Figure 4. Effect of input feed rate on (A) number of blade passes and (B) mean centered variance.

[Color figure can be viewed in the online issue, which is available at wileyonlinelibrary.com.]

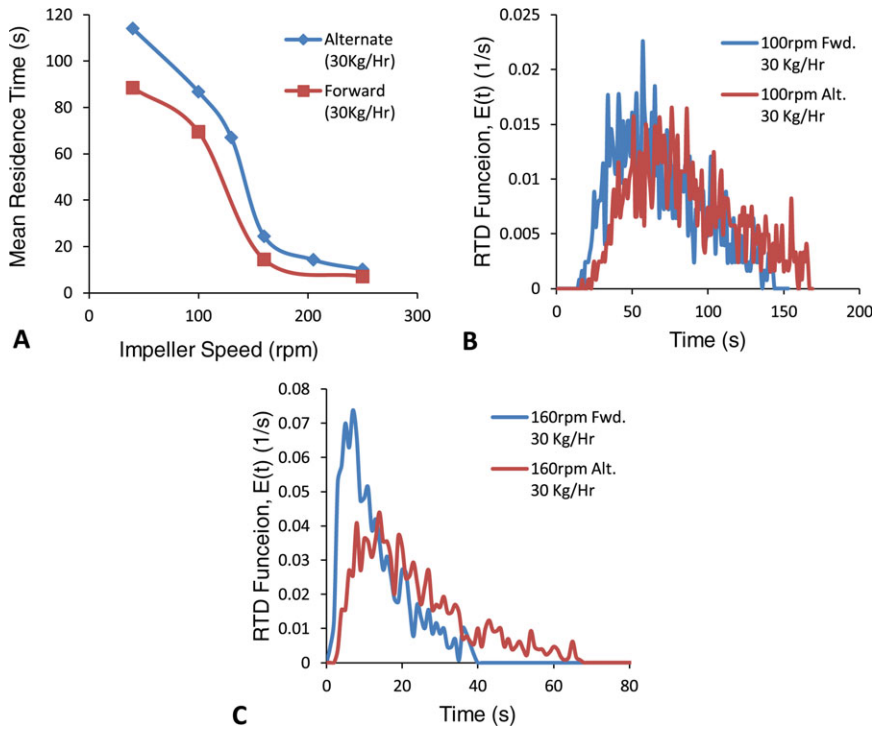

Figure 5. Effect of impeller design (forward- and alternating-blade angles) on (A) mean residence time; (B) RTD (100 rpm); and (C) RTD (160 rpm).

[Color figure can be viewed in the online issue, which is available at wileyonlinelibrary.com.]

the $E(t)$ plots (moving average of four points shown for clarity) at 100 and 160 rpm, respectively. The distributions for the two blade patterns are different and the difference is more pronounced at higher speed. At 160 rpm, the $E(t)$-plot for the forward blade pattern resembles that of a fluidized state, whereas it is not quite the case for the alternating-blade pattern. The alternate-blade design results in a much wider RTD. The plots at other speeds are not shown as they follow the same pattern.

Both blade patterns follow the humped profile for the number of blade passes but the alternate design resulted in higher number of blade passes at all speeds (Figure 6A). In blenders that allow changes in blade angles, this knowledge can be used to tweak the ratio of forward- to backward-facing blades for desired shear. Finally, the mean centered variance (Figure 6B) was higher for forward blade design at speeds ranging from 100–160 rpm. The impeller design had no impact on the variance at 40 rpm. At speeds more than 200 rpm, however, the alternate blade pattern produced higher variance.

It is interesting to consider that for other mixing applications dealing with liquids and suspensions (i.e., stirred tanks, static mixers, and extruders) the equipment manufacturers have spent enormous amounts of time and energy developing geometric designs that optimize performance. No such work exists today for continuous powder blenders. As the results presented here indicate, the development of this technology is at its infancy, and we anticipate substantial efforts in the future will be devoted to optimizing the geometry of these systems.

Comparison between simulations and experiments

To assess the usability of DEM simulations in predicting performance of real-world continuous blending processes, a

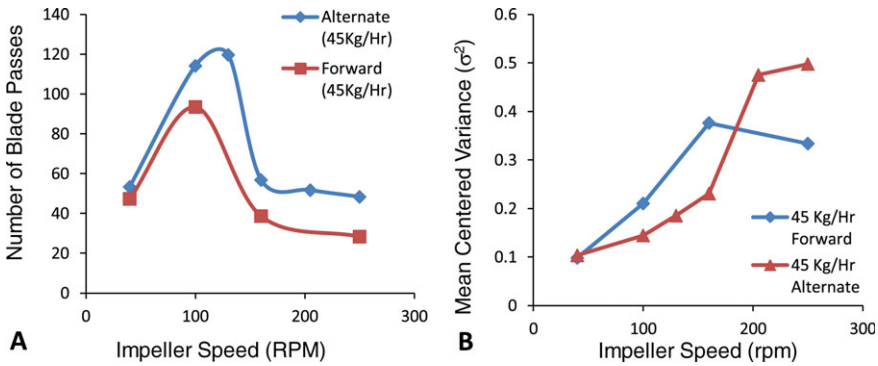

Figure 6. Effect of impeller design (forward and alternating blade angles) on (A) number of blade passes and (B) mean centered variance.

[Color figure can be viewed in the online issue, which is available at wileyonlinelibrary.com.]

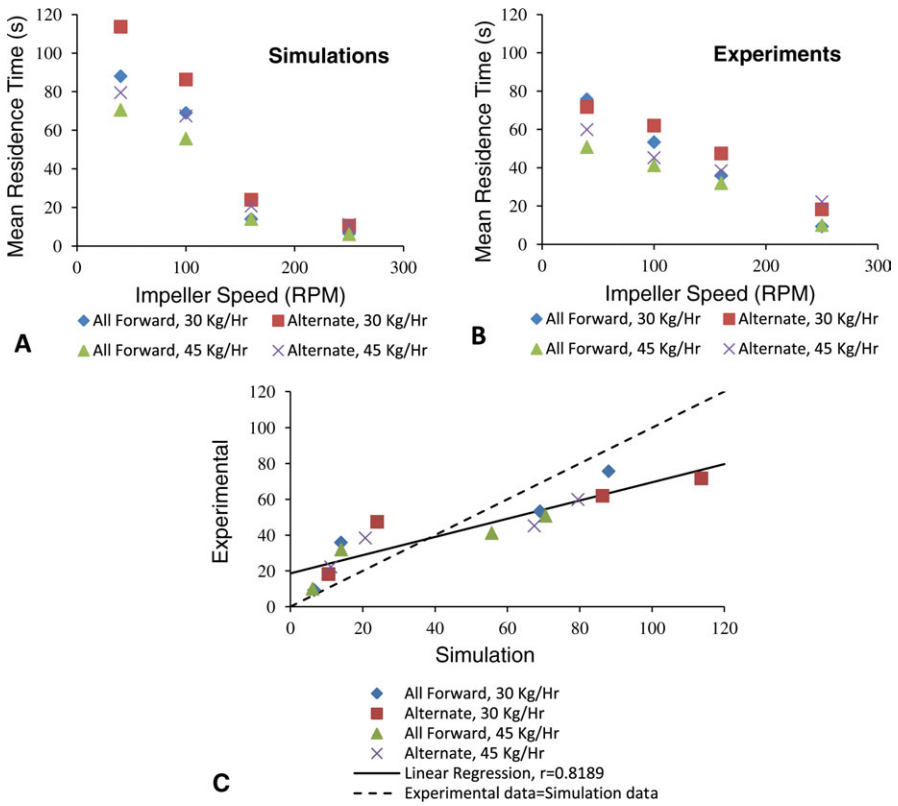

Figure 7. (A and B) Comparison between the trends observed for mean residence time as a function of process parameters (feed rate, impeller speed) and impeller designs and (C) experimental values of mean residence time are compared with values computed from DEM simulations.

[Color figure can be viewed in the online issue, which is available at wileyonlinelibrary.com.]

comparison was made between the experimental measurements and responses computed from the simulation data. Number of blade passes, mean residence time, and mean centered variance were chosen as the variables for the comparison. Details on experimental methods and materials used can be found in Vanarase and Muzzio.[46] The geometric design of the blender used in both studies was identical.

Mean Residence Time. The trends observed for mean residence time as a function of impeller speed, feed rate, and impeller design showed a good qualitative agreement (Figure 7A, B). In both simulations and experiments, mean residence time decreased as function of impeller speed, decreased as function of feed rate and was higher for alternating-blade configuration than the forward-blade design. Further, the relative interactions between all the parameters in either simulations or experiments were captured accurately. However, as expected, quantitative comparison between the two methods showed some differences that can be attributed to limitations of the model (approximate contact dynamics, much larger particle size, strictly spherical particle shape, neglected effects of surrounding air, etc.).

Figure 7C shows a one-to-one quantitative comparison. The experimental values were higher than simulation values in the lower range of residence times, whereas opposite behavior was observed in the higher range. Lower values of residence times (0–30 s, *X* axis) belong to the impeller speed of 250 rpm. The numerical calculations are performed at a frequency small enough to capture essential dynamics and large enough so that the simulations are feasible time-wise. At such a high speed, the overlaps on particle–blade and interparticle impacts are larger than those at low speed simulations. As a result, the normal forces experienced by a particle on impact are significantly higher leading to a faster exit from the blender. Furthermore, in the experiment the blades get coated by powder which may further reduce the coefficient of restitution. The higher values of mean residence times (50–120 s, *X* axis) correspond to the impeller speeds of 40–160 rpm. At these speeds, particles are not completely fluidized and there is significant amount of tangential rolling/slippage occurring between particles and impeller blades in the simulation, which leads to higher residence time than in the experiment.

Number of blade passes. As shown in Figure 8, qualitatively, the effects of feed rate and impeller design were similar in both experiments and simulations. The simulations showed a peak in N_p at a speed of around 130 rpm (also explained in Figure 2C), whereas the experiments predicted the peak to appear around 160 rpm.

Mean centered variance. The mean centered variance showed poor qualitative agreement between the experimental and the simulation results (Figure 9). It is an indicator of dispersive action of the mixer. The mean centered variance is a combined result of convection and random movement of particles. Because of computational limitations, diffusive component was not captured well by the simulations.

This comparison indicates that DEM simulations can prove to be an excellent tool in predicting qualitative trends, which can be further improved with enhancements in the model (such as inclusion of realistic particle size, shape, properties such as cohesion and the effects of air) and fine-tuning of material properties.

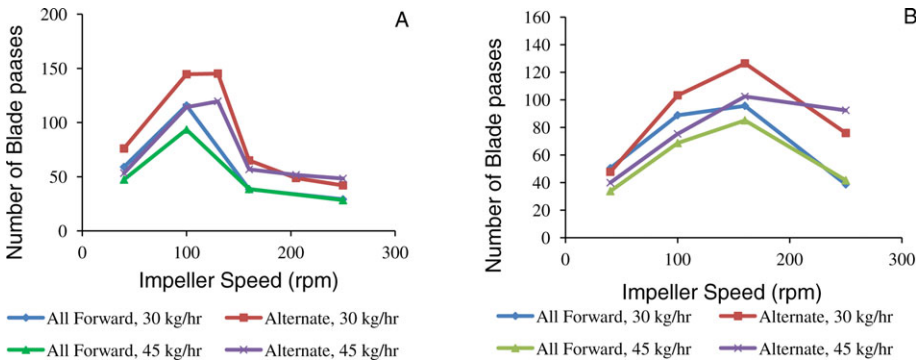

Figure 8. Comparison between the trends observed for number of blade passes as a function of process parameters (feed rate, impeller speed) and impeller designs.

[Color figure can be viewed in the online issue, which is available at wileyonlinelibrary.com.]

Conclusions and Discussion

Computer simulation of a continuous mixer was performed using DEM. The effects of impeller speed, input feed rate and impeller design were studied using critical performance indicators namely the mean residence time (τ), the RTD, the number of blade passes (N_p) and the mean centered variance (σ^2). It was found that the mixer performance could be classified into two classes: the prefluidization and postfluidization states. Furthermore, the effects of the parameters studied were not entirely independent of each other and hence must be studied in conjunction.

The primary effect of increase in impeller speed was to reduce the hold-up as well as the amount of time the powder spends in the blender. In the prefluidization states, the mean residence time dropped sharply with increasing speed. The rate of decrease was found to be feed-rate dependent. In the postfluidization regime, the changes were less prominent regardless of the feed rates. Increasing impeller speed also showed different RTDs among the tracer particles. At low–intermediate speeds of 40–130 rpm, the distributions were wide and they progressively narrowed at higher speeds of 160–250 rpm. The number of blade passes, a measure of the shear experienced by the powder, changed considerably with speed, with a peak right before fluidization (100–130 rpm). They did not change appreciably postfluidization. At a given impeller speed, the numbers were higher for lower feed rates. The dispersion produced by the mixer was quantified using the mean centered variance. It showed an increasing trend with impeller speed up to a point and then dropped. The inflection point was dictated by the feed rate. The highest speed did not create the largest dispersion even though the largest fluidization was observed at this speed.

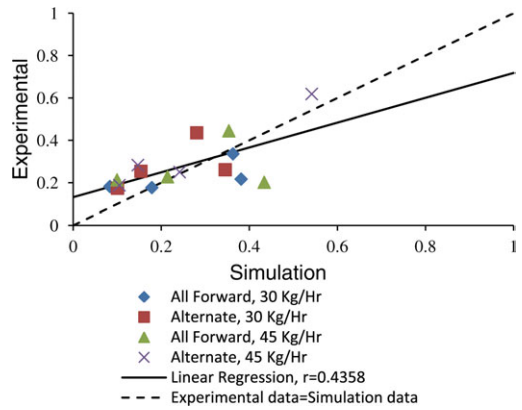

Figure 9. Experimental values of mean centered variance are compared with values computed from DEM simulations.

[Color figure can be viewed in the online issue, which is available at wileyonlinelibrary.com.]

The mean residence time decreased with increasing feed rate although the effect was only noticeable in prefluidization regimes. The RTD showed a similar effect—increase in feed rate produced narrower $E(t)$-curves in the prefluidization regime. The distributions were similar to each other postfluidization. In other words, the particles spent lesser time in the blender and the RTD among them was likely to be more uniform for a higher feed rate if the blender was operated on lower speeds. The feed rate had a significant effect on the number of blade passes. The operating range of 100–130 rpm was found to produce the highest number of blade passes for all feed rates. However, the highest feed rate resulted in similar number of blade passes at all other speeds indicating that if it is desirable to keep the amount of shear constant, then a higher feed rate may allow for a broader operating range of impeller speeds. The prefluidization regimes showed higher mean centered variance at lower feed rates but the trends reversed after 160 rpm.

The alternating-blade pattern with some backward facing blades produced higher holdups and mean residence times than the forward-facing blade pattern. The difference in the RTD was more pronounced at higher speeds. The alternate blade set resulted in a significantly larger number of blade passes at all speeds except 40 rpm. In the prefluidization regime, the forward blade pattern produced higher dispersion, whereas the opposite was true postfluidization.

Experimental studies showed that the simulations captured the effects of the critical parameters well. A quantitative agreement will be difficult to achieve given the limitations of model and computational resources. However, this type of simulation can be used to reduce the number of experiments and the model can be extended to study aspects which are not easy to derive experimentally such as finding regions of high shear within the blender, optimizing the device design, and so forth.

Literature Cited

1. Muzzio FJ, Shinbrot T, Glasser BJ. Powder technology in the pharmaceutical industry: the need to catch up fast. *Powder Technol.* 2002;124):1–7.
2. Moakher M, Shinbrot T, Muzzio FJ. Experimentally validated computations of flow, mixing and segregation of non-cohesive grains in 3D tumbling blenders. *Powder Technol.* 2000;109:58–71.

3. Lemieux M, Bertrand F, Chaouki J, Gosselin P. Comparative study of the mixing of free-flowing particles in a V-blender and a bin-blender. *Chem Eng Sci*. 2007;62:1783–1802.
4. Lemieux M, Léonard G, Doucet J, Leclaire LA, Viens F, Chaouki J, Bertrand F. Large-scale numerical investigation of solids mixing in a V-blender using the discrete element method. *Powder Technol*. 2008;181:205–216.
5. Sudah OS, Coffin-Beach D, Muzzio FJ. Quantitative characterization of mixing of free-flowing granular material in tote (bin)-blenders. *Powder Technol*. 2002;126:191–200.
6. Arratia PE, Duong N-h, Muzzio FJ, Godbole P, Reynolds S. A study of the mixing and segregation mechanisms in the Bohle Tote blender via DEM simulations. *Powder Technol*. 2006;164:50–57.
7. Brone D, Muzzio FJ. Enhanced mixing in double-cone blenders. *Powder Technol*. 2000;110:179–189.
8. Dubey A, Sarkar A, Ierapetritou M, Wassgren CR, Muzzio FJ. Computational Approaches for Studying the Granular Dynamics of Continuous Blending Processes, 1 – DEM Based Methods. *Macromol Mater Eng*. 2011;296:290–307.
9. Chaudhuri B, Mehrotra A, Muzzio FJ, Tomassone MS. Cohesive effects in powder mixing in a tumbling blender. *Powder Technol*. 2006;165:105–114.
10. Zhu RR, Zhu WB, Xing LC, Sun QQ. DEM simulation on particle mixing in dry and wet particles spouted bed. *Powder Technol*. 2011;210:73–81.
11. Bertrand F, Leclaire LA, Levecque G. DEM-based models for the mixing of granular materials. *Chem Eng Sci*. 2005;60:2517–2531.
12. Faqih A, Chaudhuri B, Alexander AW, Davies C, Muzzio FJ, Silvina Tomassone M. An experimental/computational approach for examining unconfined cohesive powder flow. *Int J Pharm*. 2006;324:116–127.
13. Zhu HP, Zhou ZY, Yang RY, Yu AB. Discrete particle simulation of particulate systems: a review of major applications and findings. *Chem Eng Sci*. 2008;63:5728–5770.
14. Finnie GJ, Kruyt NP, Ye M, Zeilstra C, Kuipers JAM. Longitudinal and transverse mixing in rotary kilns: a discrete element method approach. *Chem Eng Sci*. 2005;60:4083–4091.
15. Marigo M, Cairns DL, Davies M, Ingram A, Stitt EH. Developing mechanistic understanding of granular behaviour in complex moving geometry using the discrete element method. Part B: investigation of flow and mixing in the Turbula® mixer. *Powder Technol*. 2011;212:17–24.
16. Johnson PC, Jackson R. Frictional & collisional constitutive relations for granular materials, with application to plane shearing. *J Fluid Mech Digital Arch*. 1987;176:67–93.
17. Mehta A, Edwards SF. A phenomenological approach to relaxation in powders. *Phys A: Stat Theoret Phys*. 1990;168:714–722.
18. Lakehal D, Narayanan C. Numerical analysis of the continuum formulation for the initial evolution of mixing layers with particles. *Int J Multiphase Flow*. 2003;29:927–941.
19. Doucet J, Hudon N, Bertrand F, Chaouki J. Modeling of the mixing of monodisperse particles using a stationary DEM-based Markov process. *Computers & Chemical Engineering*. 2008;32:1334–1341.
20. Fan LT, Too JR, Nassar R. Stochastic simulation of residence time distribution curves. *Chem Eng Sci*. 1985;40:1743–1749.
21. Ponomarev D, Mizonov V, Gatumel C, Berthiaux H, Barantseva E. Markov-chain modelling and experimental investigation of powder-mixing kinetics in static revolving mixers. *Chem Eng Process: Process Intensification*. 2009;48:828–836.
22. Boukouvala F, Dubey A, Vanarase AU, Ramachandran R, Muzzio FJ, Ierapetritou MG. Computational approaches for studying the granular dynamics of continuous blending processes. II: population balance and data-based methods. *Macromol Mater Eng*. 2012;297:9–19.
23. Portillo PM, Muzzio FJ, Ierapetritou MG. Hybrid DEM-compartment modeling approach for granular mixing. *AICHE J*. 2007;53:119–128.
24. Hawkesworth MR, Parker DJ, Fowles P, Crilly JF, Jefferies NL, Jonkers G. Nonmedical applications of a positron camera. *Nucl Instrum Meth A*. 1991;310:423–434.
25. Parker DJ, Broadbent CJ, Fowles P, Hawkesworth MR, McNeil P. Positron emission particle tracking—a technique for studying flow within engineering equipment. *Nucl Instrum Meth A*. 1993;326:592–607.
26. Kuo HP, Knight PC, Parker DJ, Tsuji Y, Adams MJ, Seville JPK. The influence of DEM simulation parameters on the particle behaviour in a V-mixer. *Chem Eng Sci*. 2002;57:3621–3638.
27. Cleary PW, Metcalfe G, Liffman K. How well do discrete element granular flow models capture the essentials of mixing processes? *Appl Math Model*. 1998;22:995–1008.
28. Kwapinska M, Saage G, Tsotsas E. Mixing of particles in rotary drums: a comparison of discrete element simulations with experimental results and penetration models for thermal processes. *Powder Technol*. 2006;161:69–78.
29. Berthiaux H, Marikh K, Gatumel C. Continuous mixing of powder mixtures with pharmaceutical process constraints. *Chem Eng Process: Process Intensification*. 2008;47:2315–2322.
30. Portillo PM, Ierapetritou MG, Muzzio FJ. Characterization of continuous convective powder mixing processes. *Powder Technol*. 2008;182:368–378.
31. Sarkar A, Wassgren C. Continuous blending of cohesive granular material. *Chem Eng Sci*. 2010;65:5687–5698.
32. Sarkar A, Wassgren CR. Simulation of a continuous granular mixer: effect of operating conditions on flow and mixing. *Chem Eng Sci. 1* 2009;64:2672–2682.
33. Cundall PA, Strack ODL. A discrete numerical model for granular assemblies. *Geotechnique*. 1979;29:47–65.
34. Gao Y, Vanarase A, Muzzio F, Ierapetritou M. Characterizing continuous powder mixing using residence time distribution. *Chem Eng Sci*. 2011;66:417–425.
35. Portillo PM, Ierapetritou MG, Muzzio FJ. Effects of rotation rate, mixing angle, and cohesion in two continuous powder mixers—A statistical approach. *Powder Technol*. 2009;194:217–227.
36. Tsuji Y, Tanaka T, Ishida T. Lagrangian numerical simulation of plug flow of cohesionless particles in a horizontal pipe. *Powder Technol*. 1992;71:239–250.
37. Hertz H. On the contact of elastic solids. *J. Reine Angew Math*. 1882;92:156–171.
38. Mindlin RD, Deresiewicz,H. Elastic spheres in contact under varying oblique forces. *ASME J Appl Mech*. 1953;20:327–344.
39. Remy B, Canty TM, Khinast JG, Glasser BJ. Experiments and simulations of cohesionless particles with varying roughness in a bladed mixer. *Chem Eng Sci*. 2010;65:4557–4571.
40. Metzger MJ, Remy B, Glasser BJ. All the Brazil nuts are not on top: vibration induced granular size segregation of binary, ternary and multi-sized mixtures. *Powder Technol*. 2011;205:42–51.
41. Gyenis J, Ulbert Z, Szépvölgyi J, Tsuji Y. Discrete particle simulation of flow regimes in bulk solids mixing and conveying. *Powder Technol*. 1999;104:248–257.
42. Limtrakul S, Boonsrirat A, Vatanatham T. DEM modeling and simulation of a catalytic gas-solid fluidized bed reactor: a spouted bed as a case study. *Chem Eng Sci*. 2004;59:5225–5231.
43. Limtrakul S, Chalermwattanatai A, Unggurawirote K, Tsuji Y, Kawaguchi T, Tanthapanichakoon W. Discrete particle simulation of solids motion in a gas-solid fluidized bed. *Chem Eng Sci*. 2003;58:915–921.
44. Kruggel-Emden H, Simsek E, Rickelt S, Wirtz S, Scherer V. Review and extension of normal force models for the discrete element method. *Powder Technol*. 2007;171:157–173.
45. Kruggel-Emden H, Wirtz S, Scherer V. A study on tangential force laws applicable to the discrete element method (DEM) for materials with viscoelastic or plastic behavior. *Chem Eng Sci*. 2008;63:1523–1541.
46. Vanarase AU, Muzzio FJ. Effect of operating conditions and design parameters in a continuous powder mixer. *Powder Technol*. 2011;208:26–36.
47. Danckwerts PV. Continuous flow systems. Distribution of residence times:. *Chem Eng Sci*. 1953;2:1–13.
48. Sudah OS, Chester AW, Kowalski JA, Beeckman JW, Muzzio FJ. Quantitative characterization of mixing processes in rotary calciners. *Powder Technol*. 2002;126:166–173.
49. Pingali K, Mendez R, Lewis D, Michniak-Kohn B, Cuitiño A, Muzzio F. Evaluation of strain-induced hydrophobicity of pharmaceutical blends and its effect on drug release rate under multiple compression conditions. *Drug Dev Ind Pharm*. 2011;37:428–435.
50. Mendez R, Muzzio FJ, Velazquez C. Powder hydrophobicity and flow properties: effect of feed frame design and operating parameters. *AICHE J*. 2012;58:697–706.

Manuscript received Nov. 11, 2011, and revision received Jan. 31, 2012.